

Adsorption of Orange G Dye from Aqueous Solutions Using Magnesium Oxide Nanoparticles

Amir Fahdil, Dawood AL-Niaimi, Abdulilah.Ahmed Olaiwy*

Received: 12 June 2018 / Received in revised form: 20 August 2018, Accepted: 22 August 2018, Published online: 24 August 2018
© Biochemical Technology Society 2014-2018
© Sevas Educational Society 2008

Abstract

Magnesium Oxide (MnO₂) nanoparticles were synthesized by Hydrothermal method. The synthesized samples were characterized using FT-IR, X-ray diffraction, AFM, and SEM. The adsorption of Orange G dye from aqueous solution onto MnO₂ as adsorbent by batch method, under various experimental conditions including exposure time, MnO₂ dosage, pH, temperature, and initial Orange G dye concentration was investigated. Adsorption isotherms were used to test the adsorption data for Langmuir, Freundlich, Dubinin and Temkin as it was fit to Langmuir isotherm and type S according to Gilles' classification. Thermodynamic functions' data such as ΔH° , ΔG° , and ΔS° of the adsorption process were calculated, which showed that the adsorption endothermic process and the value of ΔG° was negative. This indicate that the adsorption happened spontaneously. The value of ΔS° is positive, which means the movement of dye molecules is unrestricted. Kinetic data were fit to pseudo-second order model.

Keywords: Adsorption, Orange G, MnO₂, Thermodynamics, kinetic study.

Introduction

Dyes are widely used in industries such as textile, leather, food, and plastic materials (Li et al. 2012). The waste water of industrial activities contains a variety of potentially toxic and environmentally harmful compounds. These compounds present an increasingly serious threat to human and environmental health (Tiwari et al. 2013). Most of the dyes are stable in nature when exposed to light and oxidizing agents (Wang et al. 2010). Various methods such as biodegradation (Kalyani et al. 2009), advanced oxidation (Ghoneim et al. 2011), ultrafiltration (Deriszadeh et al. 2010), and adsorption (Luo et al. 2010) have been applied to remove dyes from aqueous solutions. Adsorption has gained increased attention in removing dyes because of its simplicity, high efficiency, minimization of chemical sludge, and regeneration of adsorbents. A wide variety of adsorbents, have been used to remove dyes from aqueous solutions including activated carbon, zeolite (Meshko et al. 2001), perlite (Doğan and

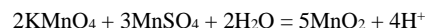
Alkan 2003), chitin (Mckay et al. 1982), lemon peel (Kumar 2007). Manganese dioxide (MnO₂) is one of the most stable compounds with excellent physical and chemical properties under ambient conditions (Zordan and Hepler 1968; Zhang, 2008; Cheng et al. 2006; Subramanian et al. 2008; Pang et al. 2012).

Experimental

Instruments: UV-Visible (Shimadzu, Japan 1700) was used to measure the dye concentration in aqueous solution. The pH of all solutions was recorded by pH meter 7110 wtw, Germany. The temperature was controlled using isothermal water bath shaker (BS-11, Korea). MnO₂ was measured using XRD (XRD-6000; Shimadzu company, Japan) with CuK α radiation of $\lambda = 0.15406$ nm. The measurement conditions of XRD were 40 kv, 30 mA, with the scanning range of 10-80° and the scanning speed of 5 deg/min. FTIR (Shimadzu, IR PRESTIGE 21) was performed with KBr pellet technique, and the effective range was from 4000 to 400 cm⁻¹. AFM (SPM-AA3000, Advanced Angstrom Inc.) and SEM (Type Tescan Brno-Mira 3LMU) were also used. All of the chemicals were used without further purification.

Synthesis of MnO₂

MnO₂ nanoparticles were synthesized by mixing aqueous solution of KMnO₄ and MnSO₄ at ambient temperature and pressure; the pH of solution mixture was adjusted ≈ 1 with concentrated HNO₃. 1.84 g of KMnO₄ (dissolved in 31.25 ml H₂O) was mixed with 2.75 g of MnSO₄ (dissolved in 9.5 ml H₂O) at ambient temperature and pressure. Concentrated HNO₃ was added to the reaction vessel to adjust the pH to ≈ 1 . The reaction product was then incubated at 80 °C for 24 hours, filtered, washed with water until the pH reached 6, and dried at 110 °C (Pang et al. 2012; Xiao et al. 1998).



Synthesis of Orange G solution

Orange G is water soluble (λ max 478 nm). A standard solution (1000 mg/L) was prepared by dissolving 1 g of Orange G dye in 1 L of DI water. The experimental solution was prepared by diluting

Amir Fahdil, Dawood AL-Niaimi, Abdulilah.Ahmed Olaiwy*

Department of Chemistry, College of Science, University of Diyala, Diyala, Iraq.

*Email: bdalaha 725 @ gmail . com

the standard solution of dye with DI water to obtain the appropriate concentration of the desired solutions (5-30 ppm), and the solutions were left for 24 hours in order to homogenize. Diluted HCl (0.1 M) and NaOH (0.1 M) were used for pH adjustment. The UV-Visible spectrometer used to determine calibration curve for Orange G dye at λ_{max} 478 nm. The dye adsorption was evaluated by batch process with different parameters such as contact time (25-125 min), dose of adsorbed MnO₂ (0.01-0.05 g), pH (3-10), concentration of dye (5-30 ppm), and temperature (20- 40°C). The samples were shaken and kept in a thermostat for 2 h, filtered in a centrifuge for 15 min at 3500 rpm, filtered again, and analyzed spectrophotometrically. The percentage of dye adsorption from the aqueous solution was determined according to the following equation (Bykkam et al. 2013):

$$\% \text{ Adsorption} = \frac{C_o - C_e}{C_o} \times 100 \quad (1)$$

Where C_o and C_e (both mg/L), are the initial concentration and the concentration at any time, respectively. The adsorption capacity Q_e (mg/g) was calculated as follows:

$$Q_e = \frac{C_o - C_e}{m} \cdot V_{sol} \quad (2)$$

Q_e: Amount of solute adsorbed per unit weight of adsorbent (mg/g); C_e: Equilibrium concentration of solute (mg/L); V_{sol}: Volume of solution (L); m: mass of adsorbent (g).

Results and Discussion

Characterization of MnO₂

In order to investigate the functional groups of MnO₂, FT-IR spectroscopy was used in the wave number range of 4000- 400 cm⁻¹ (Figure 1). At this range the bands at 524 and 462 cm⁻¹ assigned to Mn-O vibration of MnO₂ Nano powder. The bands at 3354 and 1647 cm⁻¹ can be assigned to OH stretching vibration and bending vibration of adsorbed H₂O (because of high surface-to-volume ratio in nano-crystalline materials).

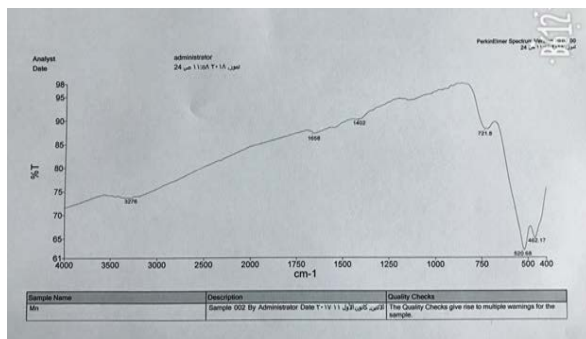


Figure 1: FTIR spectra of MnO₂

Figure (2) shows all diffraction data are in good agreement with JCPDS files No. 00-044-0141. The diffraction peaks are sharp and the crystal grows completely with high purity and with good

agreement with ref. (16). From peak at $2\theta = 28.55$, particle size for α - MnO₂ has been calculated by using Debye-Scherer's Equation $D = 0.9 \lambda / \beta \cos \theta = 8.1 \text{ nm}$.

The strongest three peaks were 2θ , 28.55° (FWHM=1.02,1/11=100), 37.41° (FWHM=0.6467,1/11=88), and 12.61° (FWHM=0.6600,1/11=44). Other peaks appeared at $2\theta = 13.26^\circ, 17.9^\circ, 36.47^\circ, 41.76^\circ, 49.61^\circ,$ and 68° . Peaks of a tetragonal α - MnO₂ phase showed a complete phase transformation of δ - MnO₂ into α - MnO₂ phase upon aging at 80 °C for 24 hours. Such transformation could be associated with the simultaneous morphological transformation from spherical nanoparticles to nano-rods during prolonged aging at 80°C.

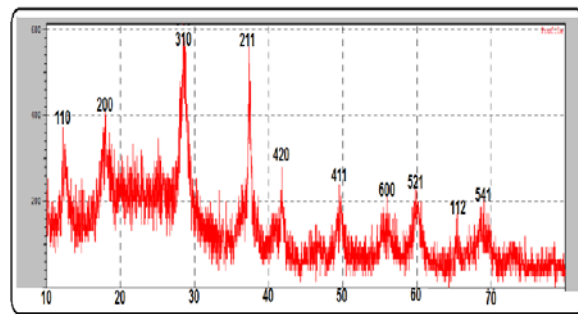


Figure 2: XRD pattern of MnO₂ nanoparticles

Atomic force microscopy (AFM) is a powerful characterization tool for determination of the particle size and surface organization of the synthesized materials. The wetting ability of a surface depends on its chemical composition, and also on the topography of the surface. MnO₂ was characterized by two- and three-dimensional AFM images, and particle size distribution for adsorbent surface was represented in figures (3, 4). The average diameter of the particle for MnO₂ was 58.48 nm; 50% with average diameter of 55 nm, 90% with average diameter of 65 nm, and the height of the sample was 1.1 nm (Fig. 3). AFM image of molecular nano-rods showed that the length is 71 nm, the width about 0.41 nm and its height 0.32 nm, while the AFM image to another molecular revealed the length to be 54 nm, the width 0.19 nm, and the height 0.66 nm. Figure 5 shows the SEM image of rod-like nanostructures of α - MnO₂.

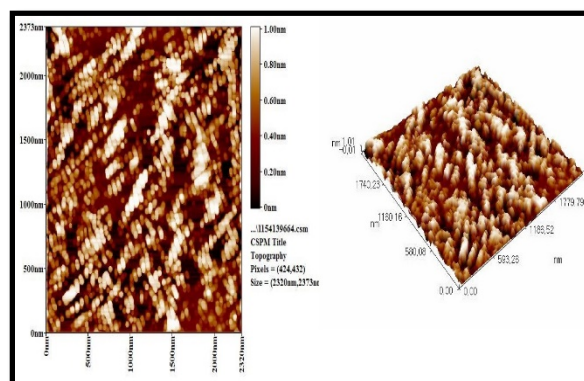


Figure 3: AFM images of MnO₂ nanoparticles

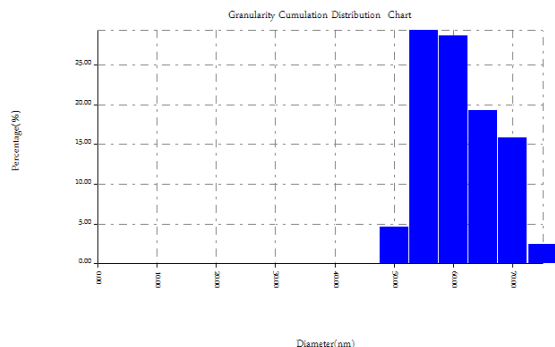


Figure 4: Particle size distribution percentage of MnO₂ nanoparticles

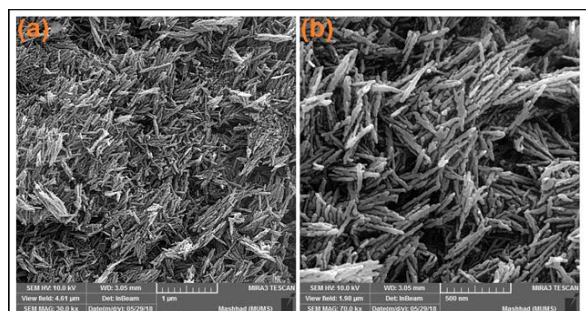


Figure 5: SEM images with different magnification power of MnO₂ nanoparticles synthesized at 80 °C for 24 hours.

Determination of Equilibrium Time of adsorption

Several adsorption experiments in contact time range of 25-125 min were performed (fig.5). The removal rate of dye onto MnO₂ gradually increased with the increase of contact time from 25 to 125 min and then remained constant (Liu et al. 2014) with further increase in contact time. Therefore, a period of 125 min of equilibrium was selected for the next studies. In the initial stage, dye contact quickly with a lot of available active sites on the surface of MnO₂, resulting in the fast adsorption. The increase of the contact time gradually lessened the available active sites, and weakened the driving force, resulting in the slow adsorption process and longer time to achieve adsorption equilibrium.

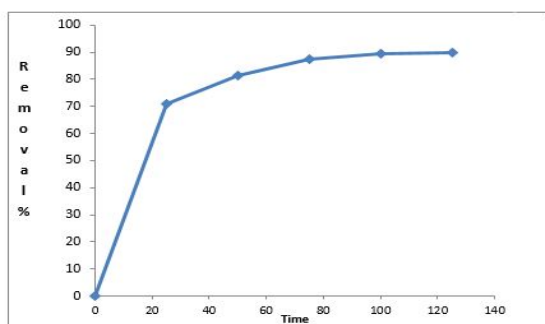


Figure 6: Effect of equilibrium time on adsorption of Orange G dye on MnO₂ nanoparticles at 25 °C, C₀= 30 ml of 10 ppm, dose of 0.04 g, and pH=8.

Effect of pH

The initial pH of the Orange G dye solution can significantly affect the adsorption capacity of the dye, because it affects the charge distribution of the surface of the adsorbent (MnO₂) as well as adsorbate (the dye molecules). Figure (7) shows that in acidic medium the adsorption capacity is maximum, and it decreases with the increase in pH.

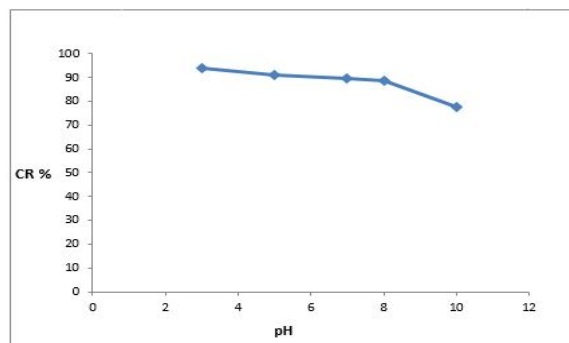


Figure 7: Effect of pH on the adsorption of Orange G dye on MnO₂ nanoparticles at 25 °C, 30 ml of 10 ppm dye, and dose 0.04 g.

Adsorbent Weight

The effect of adsorbent on removal percentage of dye was examined by taking different quantities of MnO₂ ranging from 0.01 to 0.05 g. Our results (Figure 8) showed that the best removal efficiency was obtained at 0.05 m (Smaranda et al. 2011).

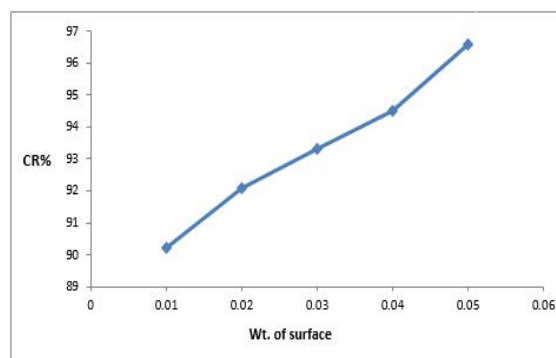


Figure 8: Effect of adsorbent weight on the adsorption of Orange G dye on MnO₂ nanoparticles at 25 °C, C₀=30 ml of 10 ppm, and pH=3.

Effect the concentration of dye on adsorption

Figure (9) shows the effect of concentration of dye (5 -30 ppm) on removal percentage of dye. Our results (figure 9) showed that the best removal efficiency was obtained at 10 ppm (Amir et al. 2017).

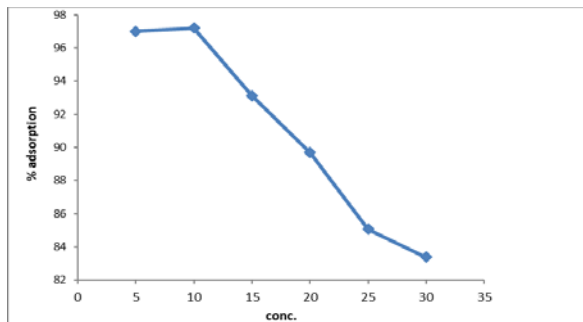


Figure 9: Effect of dye concentration on adsorption of Orange G dye on MnO₂ nanoparticles at 25 °C, dose of 0.05 g, and pH =3.

Adsorption Kinetics

In order to assess the rate of the adsorption for Orange G dye, both pseudo-first order and pseudo-second order kinetics were applied to the adsorption data (Lagergren 1898).

$$\ln (q_e - q_t) = \ln q_e - k_1 t \tag{4}$$

$$t / q_t = 1/ k_2 q_e^2 + (1/ q_e) t \tag{5}$$

Where q_e and q_t (mg/g) are the amounts of dye adsorbed at equilibrium and time t , respectively; k_1 and k_2 are the rate constant of pseudo-first order (min^{-1}) and pseudo-second order ($\text{g/mg}\cdot\text{min}$). The plots of the equations were examined for best fit by comparing their correlation coefficients (R^2). Figure 10 and 11 show the straight plots of $\ln (q_e - q_t)$ vs. t and t/q_t vs. t , respectively. The correlation coefficients of the linear curves of both kinetics show that the process more likely follows a second order kinetics. Pseudo-second order model assumes that the rate-limiting step involves chemisorption of adsorbate on the adsorbent. By fitting the experimental data (Figures 10 and 11), the adsorption rate constant for each model was calculated and summarized in Table (1). As can be seen from the table, the kinetics data were well fitted by the pseudo-second order, as demonstrated by the obtained higher regression coefficient (R^2). In addition, the calculated q_e values for the pseudo-second order is highly matched with the experimental data as compared with those of the pseudo-first order model. This indicated that the adsorption kinetics of dye on MnO₂ was not diffusion controlled (Chia et al. 2013).

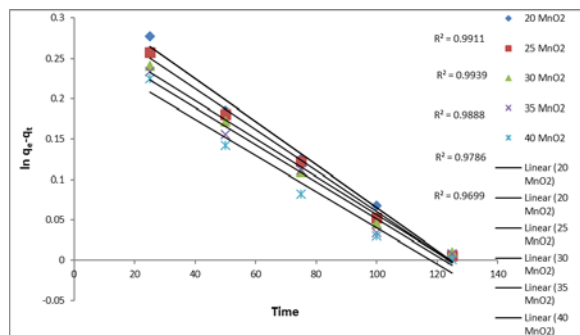


Figure 10: Plot of pseudo-first order model of Orange G dye on MnO₂ nanoparticles at different temperatures.

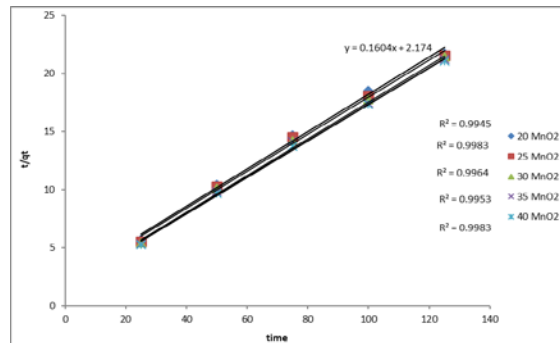


Figure 11: Plot of pseudo-second order model of Orange G dye on MnO₂ nanoparticles at different temperatures.

Table 1: Kinetics parameters for adsorption of Orange G dye on MnO₂ nanoparticles.

C ₀	T (°C)	pseudo-first -order				pseudo-second -order		
		q _e (exp.)	K ₁ (min ⁻¹)	q _e (calc.)	R ²	q _e (calc.)	K ₂ g.mg ⁻¹ .min ⁻¹	R ²
10 Ppm	20	5.78	0.0027	4.22	0.991	5.78	0.011	0.994
	25	5.83	0.0025	4.17	0.993	5.83	0.012	0.998
	30	5.88	0.0024	4.12	0.988	5.88	0.013	0.996
	35	5.93	0.0023	4.07	0.978	5.93	0.014	0.995
	40	5.94	0.0022	4.06	0.969	5.94	0.015	0.998

Adsorption Isotherm

The adsorption isotherms are to explore the relation between the adsorbate concentration in the bulk (at equilibrium) and the amount adsorbed at the surface. In this study four commonly used isotherm models (Langmuir, Freundlich, Timken, and Dubinin-Kaganer-Radushkevich) were applied to the experimental data to explain the dye-Nano (MnO₂) interaction. The Langmuir isotherm model assume monolayer coverage of the adsorbate over a homogenous adsorbent surface with identical adsorptions sites and their binding energies and neglecting any interactions between adsorbed ions, atoms or molecules (Karim et al. 2017) with each molecule adsorbed onto the surface having the same adsorption energy. The Langmuir isotherm is expressed as (Freundlich 1973):

$$\frac{C_e}{Q_e} = \frac{1}{q_{\max}K_L} + \frac{C_e}{q_{\max}} \tag{6}$$

Where C_e is the equilibrium concentration of dye (mg/L); q_{\max} , Q_e are the maximum adsorption capacity corresponding to complete monolayer coverage on the surface (mg/g) and capacity at equilibrium (mg/g), respectively; and K_L is Langmuir constant (L/mg) (Crosby 1998) related to energy of sorption. Therefore, a plot of C_e/Q_e versus C_e gives a straight line of slope $1/q_{\max}$ and intercept $(1/K_L q_{\max})$ (Figure 12). Table (2) shows that the values of q_{\max} and K_L are increased when the solution temperature increased from 20 to 40°C, which indicates that the dye is favorably adsorbed by MnO₂ at lower temperatures, which shows that the adsorption process is endothermic. A dimensionless constant separation factor of Langmuir isotherm (R_L) was also calculated using equation (Gan et al. 2015):

$$R_L = 1 / (1 + K_L C_0) \tag{7}$$

Where C_0 is the initial concentration of Orange G dye solution (mg/L) and K_L (L/mg) is the Langmuir adsorption constant given in Table (2). Table (2) explains the relation between R_L and the natural adsorption.

Table 2- Values of R_L and type of isotherm.

Value of R_L	$R_L > 1$	$R_L = 1$	$R_L < 1$	$R_L = 0$
Type of isotherm	Unfavorable	Linear	Favorable	Irreversible

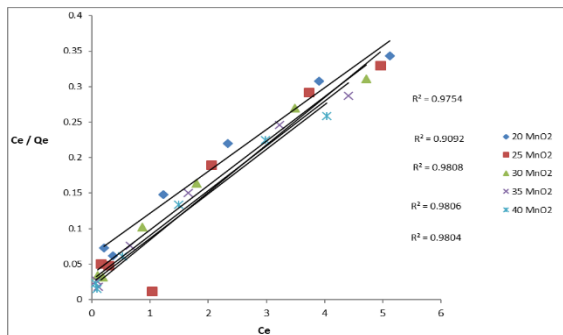


Figure 12: Isotherm Langmuir for Orange G dyes on MnO₂ nanoparticles at 25 °C.

The Freundlich model is a case for multilayer adsorption and adsorption on heterogeneous surface energies, and it gives an exponential distribution of active sites. The linear form of this model is represented by:

$$\ln Q_e = \ln K_F + 1/n \ln C_e \tag{8}$$

The Freundlich constants K_F and n indicate the adsorption capacity and the adsorption intensity are calculated from the intercept and slope of plot $\ln Q_e$ versus $\ln C_e$, respectively (Figure 13). The intensity of adsorption (n) showed low values ($n < 1$); this indicates a very low affinity between adsorbents and adsorbate. The Freundlich constant (K_F) decreases with increasing the temperature, and this is an indication for exothermic reaction. The values of n larger than 1 represent a favorable removal condition (Fungaro et al. 2011).

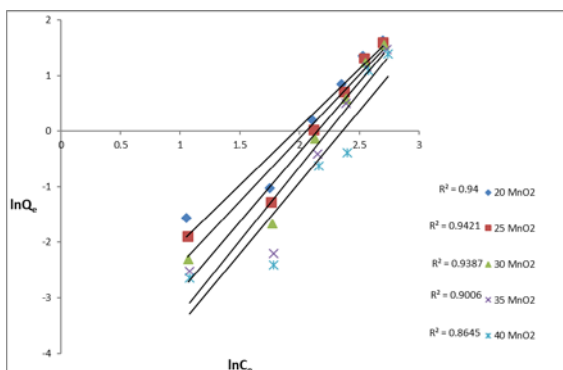


Figure 13: Isotherm Freundlich for Orange G dyes at different concentrations and 25 °C on MnO₂ nanoparticles.

A more common isotherm than Langmuir is the Dubinin-Kaganer–Radushkevich (DKR) model proposed by Dubinin, which does not assume a homogenous surface of sorbent. It is applied to determine the adsorption mechanism (physical or chemical). The linear form of (DKR) is as follows (Stoeckli 1998):

$$\ln Q_e = \ln q_{max} - \beta \epsilon^2 \tag{9}$$

Where q_{max} is the maximum sorption capacity (mg/g), β is the activity coefficient related to mean sorption energy (mol^2/J^2), and ϵ is the Polanyi potential defined as:

$$\epsilon = RT \ln (1 + 1/C_e) \tag{10}$$

Where R is the gas constant (KJ/mol. K). The slope of the plot of $\ln q_e$ versus ϵ^2 gives β and the intercept yields the sorption capacity q_{max} , as shown in Figure (14). Prediction of the adsorption mechanism (physical or chemical) can be done by calculating the value of the mean sorption energy, E (J/mol), from the following equation (Mall et al. 2006):

$$E = (-2 \beta)^{-0.5} \tag{11}$$

The values of β , q_{max} , E and R^2 as a function of temperature are listed in Table (3). If the values of E were less than 8 kJ/mol, the mechanism maybe a physical adsorption, while E values between 8-16 kJ/mol assumes the adsorption to be controlled by ion exchange, and E greater than 16 kJ/mol presume a particle diffusion mechanism (chemical process). It can be observed that the values of E may be physical (electrostatic) in nature.

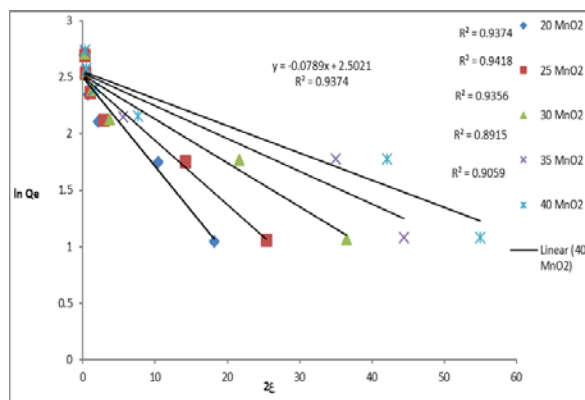


Figure 14: Isotherm Dubinin (DKR) for Orange G dye at 25 °C and different concentrations on MnO₂ nanoparticles.

The Temkin isotherm in the linear form has been used as the following equation:

$$Q_e = B \ln K_T + B \ln C_e \tag{12}$$

Where $B = RT/b$ is related to heat of adsorption (J/mol), K_T is equilibrium binding constant (L/gm), and R is the gas constant (8.314 J/mol. K). Both K_T and B are calculated (as shown in Table

3) from the intercept and the slope of curve between $\ln C_e$ and Q_e as in Figure (15).

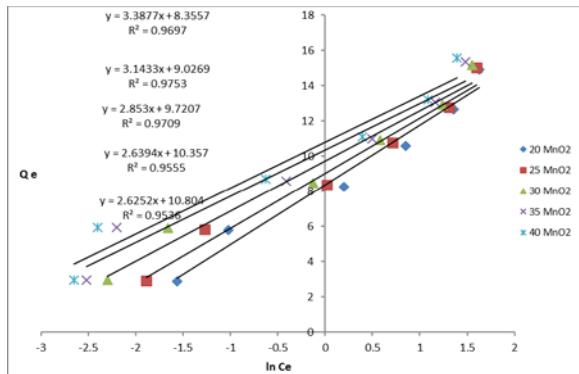


Figure 15: Isotherm Temkin for Orange G dye at 25 °C and different concentrations on MnO₂ nanoparticles.

Table 3- The calculated adsorption parameters of the four used isotherms.

T(C°)	Langmuir				Freundlich		
	K _L	R ²	q _{max}	R _L	² R	1/n	K _F
20	0.9319	0.9754	5.78	0.0969	0.94	2.075	4.0771
25	3.6648	0.9092	5.83	0.0265	0.942	2.264	4.6568
30	1.7257	0.9808	5.88	0.0547	0.938	2.507	5.3941
35	2.3029	0.9806	5.93	0.0416	0.900	2.665	5.9685
40	2.6638	0.9804	5.94	0.0036	0.864	2.569	6.054

(DKR)				Temkin		
R ²	E	q _{max}	β	R ²	B	K _T
0.397	0.397	2.502	0.0789-	0.969	3.387	8.355
0.941	0.336	2.506	0.0567-	0.975	3.143	9.026
0.935	0.278	2.514	0.0388-	0.970	2.853	9.720
0.891	0.240	2.534	0.0289-	0.955	2.639	10.357
0.905	0.219	2.553	0.0240-	0.953	2.625	10.804

The adsorption of Orange G dye on MnO₂ nanoparticles was fit to Langmuir isotherm by higher correlation factor (R²) values (Table 3) (Farghali et al. 2013).

The values of dimensionless sorption factor (K_L) were close to zero and this is an indication for favorable adsorption. The intensity of adsorption (n) showed low values (n<1); this indicates a very low affinity between adsorbents and adsorbate (Fungaro et al. 2011). The Freundlich constant (K_F) increased with increasing the temperature and this is an indication for endothermic reaction. In isotherm Dubinin (DKR), the energy equation gives us a perception of the adsorption mechanism. E < 8 KJ /mol indicates that the physical force influence adsorption, E > 16 indicates the spread of molecules, and when E between 8 and 16 indicates that adsorption is directed by ion exchange; the value of B less than 40 kJ/mol is an indication for physical adsorption (Amir et al. 2017).

Thermodynamics parameters

The thermodynamics parameters (ΔH°, ΔG°, ΔS°) of the removal of dye on MnO₂ were calculated according to the following relations:

$$K_C = Ae^{-\Delta H/RT} \tag{13}$$

$$\ln X_m = -\frac{\Delta H}{T} + K \tag{14}$$

Where $\ln X_m$ is the natural logarithm for greatest amount adsorbed (mg/g), K is the constant of Van't Hoff equation, R is the universal gas constant (8.314.10⁻³ J/mol. K⁻¹) and T is the temperature in Kelvin.

$$\Delta G^\circ = -RT\ln K \tag{15}$$

$$K = \frac{Q_e \times m}{C_e \times V}$$

$$\Delta G^\circ = \Delta H - T\Delta S^\circ \tag{17}$$

$$\Delta S^\circ = \frac{\Delta H - \Delta G^\circ}{T} \tag{18}$$

The value ΔH° was calculated from the slope and intercept of the Van't Hoff plots (the plots of $\ln X_m$ versus 1/T) (Figure 16, Table 4) (Hacıyakupoglu et al. 2015). The value of ΔH° was positive, which means the adsorption processes is endothermic; the value of ΔG is negative indicating that the adsorbent could be happened spontaneously; and the value of ΔS is positive and that means the molecules motion aren't limited.

Table 4- Values of thermodynamic functions for adsorption Orange G dye on MnO₂ nanoparticles.

C _e (mg/L)	Thermodynamic function	20 °C	25 °C	30 °C	35 °C	40 °C
30ppm	ΔH kJ.mol ⁻¹	1.63				
	ΔG kJ.mol ⁻¹	-2.60	-2.57	-2.93	-3.19	-3.51
	ΔS J.mol ⁻¹ K ⁻¹	14.43	14.09	15.04	15.64	16.42

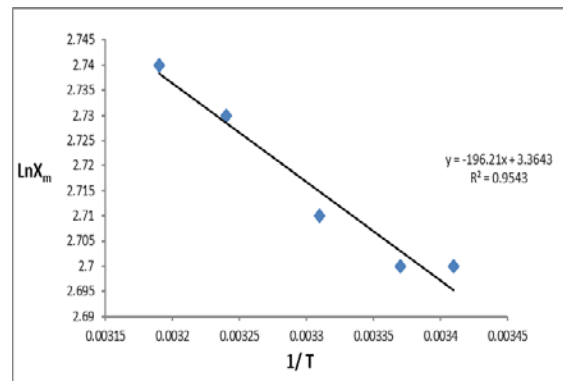


Figure 16: Values of greatest amounts adsorbed ($\ln X_m$) for Orange G dye on MnO₂ nanoparticles at different temperatures (293-318 K).

Conclusion

Based upon the experimental results of this study, nano-MnO₂ can be considered as an adsorbent for the treatment of Orange G dye

from waste water. In batch experiment, the influence of contact time, initial dye concentration, amount of MnO₂, and temperature were showed to be effective. The removal of dye is an endothermic process. It was found that the pseudo –second order model might have followed by the adsorption process as supported by correlation coefficients of the linear plots, and also $q_{e,calc}$ were very close to the $q_{e,exp}$ for the pseudo –second order rate kinetics. The isotherm study indicates four isotherms models. Adsorption data was fit to Freundlich isotherm. The Freundlich constant (k_F) increases with increasing the temperature and this is an indication for endothermic. In isotherm Dubinin (DKR), the energy equation gives us a perception of the adsorption mechanism. $E < 8$ KJ/mol indicates the physical force influence.

References

- Amir, F., Dawood, Abd, A., Khudheir, A, and Marwa, I., Mubarak, (2017). Study Eosin Dye Adsorption on the Surface Waste of Molasses Dates Production. *Diyala Journal for pure sciences*, 13(1), 22-41.
- Cheng, F.; Zhao, J.; Song, W.; Li, C.; Ma, H.; Chen, J.; Shen, P. Facile Controlled Synthesis of MnO₂ Nanostructures of Novel Shapes and Their Application in Batteries. *Inorg. Chem.* 2006, 45, 2038–2044.
- Chia, C. H., Razali, N. F., Sajab, M. S., Zakaria, S., Huang, N. M., and Lim, H. N. (2013). Methylene blue adsorption on graphene oxide. *Sains Malaysiana*, 42(6), 819-826.
- Crosby D.G. (1998). *Environmental Toxicology and Chemistry*. Oxford University Press, Oxford, 46.
- Deriszadeh, A. L. I., Husein, M. M., and Harding, T. G. (2010). Produced water treatment by micellar-enhanced ultrafiltration. *Environmental science & technology*, 44(5), 1767-1772
- Doğan, M., and Alkan, M. (2003). Adsorption kinetics of methyl violet onto perlite. *Chemosphere*, 50(4), 517-528.
- F. Stoeckli, Recent developments in Dubinins theory, *Carbon*, (1998), Vol36, No.4, pp363-368.
- Farghali, A. A., Bahgat, M., Allah, A. E., and Khedr, M. H. (2013). Adsorption of Pb (II) ions from aqueous solutions using copper oxide nanostructures. *Beni-Suef University Journal of Basic and Applied Sciences*, 2(2), 61-71.
- Fungaro, D. A., Yamaura, M., and Carvalho, T. E. M. (2011). Adsorption of anionic dyes from aqueous solution on zeolite from fly ash-iron oxide magnetic nanocomposite. *Journal of Atomic and Molecular Sciences*, 2, 305-316.
- Gan, S., Zakaria, S., Chia, C. H., Chen, R. S., & Jeyalaldeen, N. (2015). Physico-mechanical properties of a microwave-irradiated kenaf carbamate/graphene oxide membrane. *Cellulose*, 22(6), 3851-3863.
- Ghoneim, M. M., El-Desoky, H. S., and Zidan, N. M. (2011). Electro-Fenton oxidation of Sunset Yellow FCF azo-dye in aqueous solutions. *Desalination*, 274(1), 22-30.
- Haciyakupoglu, S., Orucoglu, E., Esen, A. N., Yusan, S., and Erenturk, S. (2015). Kinetic modeling of selenium (IV) adsorption for remediation of contaminated aquatic systems based on meso-scale experiments. *Desalination and Water Treatment*, 56(5), 1208-1216.
- J, N, Tiwari, N.H. Le, K.C. Kemp, R. Timilsina, K.S. Kim. (2013) Reduced graphene oxide-base hydrogels for the efficient capture of dye pollutants from aqueous solutions, *Carbon* 56, 173-182.
- J. Appel, Freundlich adsorption isotherm, *Surface Science* 39(1973) ,273-244.
- Kalyani, D. C., Telke, A. A., Dhanve, R. S., and Jadhav, J. P. (2009). Ecofriendly biodegradation and detoxification of Reactive Red 2 textile dye by newly isolated *Pseudomonas* sp. SUK1. *Journal of Hazardous Materials*, 163(2), 735-742.
- Karim, H., Hassan, & Eman, R. (2017). Preparation and Characterization of Copper Oxide Nanoparticles Used to Remove Nickel Ions from Aqueous Solution. *Diyala Journal for pure sciences*, 13(2), 217-234
- Kumar, K. V. Optimum sorption isotherm by linear and non-linear methods for malachite green onto lemon peel. *Dyes and Pigments*.2007; 74(3): 595-597.
- Lagergren, S.1898.About the theory of so- called adsorption of soluble substance. *Kungliga Svenska Vetenskapsakademiens. Handlingar*; 21:1-39
- Li, Y. H., Liu, T., Du, Q., Sun, J., Xia, Y., Wang, Z., and Wu, D. (2012). Adsorption of cationic red X-GRL from aqueous solutions by graphene: equilibrium, kinetics and thermodynamics study. *Chemical and Biochemical Engineering Quarterly*, 25(4), 483-491.
- Liu, M., Dong, F., Kang, W., Sun, S., Wei, H., Zhang, W., and Liu, Y. (2014). Biosorption of strontium from simulated nuclear wastewater by *Scenedesmus spinosus* under culture conditions: adsorption and bioaccumulation processes and models. *International journal of environmental research and public health*, 11(6), 6099-6118.
- Luo, P., Zhao, Y., Zhang, B., Liu, J., Yang, Y., and Liu, J. (2010). Study on the adsorption of Neutral Red from aqueous solution onto halloysite nanotubes. *Water research*, 44(5), 1489-1497.
- Mall, I. D., Srivastava, V. C., and Agarwal, N. K. (2006). Removal of Orange-G and Methyl Violet dyes by adsorption onto bagasse fly ash—kinetic study and equilibrium isotherm analyses. *Dyes and pigments*, 69(3), 210-223.
- Mckay, G. B. H. S., Blair, H. S., and Gardner, J. R. (1982). Adsorption of dyes on chitin. I. Equilibrium studies. *Journal of applied polymer science*, 27(8), 3043-3057.
- Meshko, V., Markovska, L., Mincheva, M., and Rodrigues, A. E. (2001). Adsorption of basic dyes on granular activated carbon and natural zeolite. *Water research*, 35(14), 3357-3366.
- S. Bykkam, V. Rao, S. Chakra and T. Thunugunta, J. of *Advanced Biotechnology and Research*, Vol 4, Issue 1, (2013), pp 142-146
- S. Pang, S. Chin and C. Ling, *Journal of Nanomaterials*, (7) 2012, AID 607870.
- Smaranda, C., Gavrilescu, M., and Bulgariu, D. (2011). Studies on sorption of Congo red from aqueous solution onto soil. *International Journal of Environmental Research*, 5(1), 177-188.

- Subramanian, V.; Zhu, H.; Wei, B. Alcohol-Assisted Room Temperature Synthesis of Different Nanostructured Manganese Oxides and Their Pseudocapacitance Properties in Neutral Electrolyte. *Chem. Phys. Lett.* 2008, 453, 242–249.
- T.D. Xiao, P.R. Strutt, M. Benaïd, H. Chen and B.H. Keart, *Nanostructured Material Journal*, (1998), Vol.10, No. 6.1051-1061.
- Wang, L., Zhang, J., Zhao, R., Li, C., Li, Y., and Zhang, C. (2010). Adsorption of basic dyes on activated carbon prepared from *Polygonum orientale* Linn: equilibrium, kinetic and thermodynamic studies. *Desalination*, 254(1), 68-74.
- Zhang, H.; Cao, G.; Wang, Z.; Yang, Y.; Shi, Z.; Gu, Z. Growth of Manganese Oxide Nanoflowers on Vertically-Aligned Carbon Nanotube Arrays for High-Rate Electrochemical Capacitive Energy Storage. *Nano Lett.* 2008, 8, 2664–2668.
- Zordan, T. A.; Hepler, L. G. Thermochemistry and Oxidation Potentials of Manganese and Its Compounds. *Chem. Rev.* 1968, 68, 737–745.